

## SYNTHESIS, CHARACTERIZATION, CRYSTAL STRUCTURE AND THEORETICAL STUDIES OF N-(2,4-DICHLOROBENZYLIDENE)-3-METHYLBENZENAMINE

Türkay AYTEKİN<sup>1,\*</sup>, Dilek ELMALI<sup>2</sup>, Halil BERBER<sup>2</sup>, Filiz ŞİŞMAN<sup>2</sup>

<sup>1</sup>Department of Physics, Science Faculty, Anadolu University, 26470 Eskişehir, Turkey

<sup>2</sup>Department of Chemistry, Science Faculty, Anadolu University, 26470 Eskişehir, Turkey

### ABSTRACT

N-(2,4-dichlorobenzylidene)-3-methylbenzenamine (**L6**) was synthesized as single crystal and characterized by FT-IR, Raman, <sup>1</sup>H NMR, <sup>13</sup>C NMR and UV-VIS spectroscopy. The thermal stability of the title compound was also studied by thermogravimetric analysis (TGA) and differential thermal analysis (DTA) analyses. The optimized geometric parameters, conformational analysis, normal mode frequencies and corresponding vibrational assignments of **L6** was theoretically examined by means of density functional theory (DFT) method using the Becke-3-Lee-Yang-Parr (B3LYP) exchange-correlation functional and the 6-311G++(d, p) basis sets. The DFT based nuclear magnetic resonance (NMR) calculations were also performed to be used for assigning the <sup>1</sup>H and <sup>13</sup>C NMR chemical shifts of **L6**. Reliable vibrational assignments were investigated by the potential energy distribution analysis and the highest occupied and the lowest unoccupied molecular orbitals (HOMO and LUMO) of **L6** was predicted. A good consistency were obtained between the theoretically predicted structural parameters, vibrational frequencies and those obtained experimentally.

**Keywords:** Nitrile, Metallophthalocyanine, Cyclotetramerization, Macrocyclic

## 1. INTRODUCTION

Hugo Schiff described the condensation between an aldehyde and an amine leading to a Schiff base in the 1860s [1]. Since then a variety of methods for the synthesis of Schiff bases have been described. Schiff base ligands may contain a variety of substituents with different electron-donating or electron-withdrawing groups and therefore may be interesting chemical properties [1]. A Schiff base is the nitrogen analogue of aldehyde in which the C=O group is replaced by a C=N group [2]. Schiff bases, also known as N-substituted imines have been widely studied as ligands in the development of organic coordination complexes of transition metals [1-3]. Schiff bases constitute one of the most widely used families of organic compounds, not only as synthetic intermediates but also in coordination chemistry [2]. Under ordinary conditions aromatic aldehydes and aromatic amines react very readily to give Schiff bases. These Schiff bases are well-defined, crystalline substances. Many studies show the biological role of Schiff bases as anticancer, antitumor, non-steroidal anti-inflammatory drugs [4-9]. The imines derived from aniline and its derivatives with aromatic aldehydes have a wide variety of applications, particularly in biological, pharmaceutical and other chemical industries [9-12]. We reported the synthesis, crystal structure, characterization and theoretical studies of Schiff base compound **L6**. The literature survey reveals that to the best of our knowledge no detailed study available on FT-IR, Raman, <sup>1</sup>H NMR, <sup>13</sup>C NMR and UV-VIS spectroscopy, single crystal and the thermogravimetric (TGA/DTA) study on **L6**.

\*Corresponding Author: [maytekin@anadolu.edu.tr](mailto:maytekin@anadolu.edu.tr)

## 2. EXPERIMENTAL SECTION

### 2.1. General

All reagents and solvents for synthesis and spectroscopic studies were purchased from Aldrich and used without any further purification. The FT-IR (4000-400  $\text{cm}^{-1}$ ) spectrum as a KBr pellet was recorded via a Bruker Optics IFS 66v/s FT-IR spectrometer with 2  $\text{cm}^{-1}$  resolution in vacuum. For the Raman spectra, the compound was recorded using a Bruker Senterra Dispersive Raman microscope spectrometer at 532 nm excitation from a 3B diode laser having 9-18  $\text{cm}^{-1}$  resolution between 3700 and 60  $\text{cm}^{-1}$  spectral region. The  $^1\text{H}$  (400 MHz;  $\text{CDCl}_3$ ) and  $^{13}\text{C}$  (100 MHz;  $\text{CDCl}_3$ ) NMR spectra were recorded on a Bruker Ultra Shield Plus-400 MHz instrument. Crystallographic data were collected on a Bruker AXS APEX [42] CCD diffractometer equipped with a rotation anode at 100 (2) K using graphite monochromated Mo  $\text{K}\alpha$  radiation ( $\lambda = 0.71073 \text{ \AA}$ ). Absorption corrections by psi-scan were applied. The data reduction was performed with the SAINT program package. Structure was solved by direct-methods and by full-matrix least squares against  $F^2$  using all data [43]. All non-hydrogen atoms were refined anisotropically. Hydrogen atoms were added to the structure model at calculated positions. Geometric calculations were performed with Platon [44]. Molecular drawings were obtained using Mercury [45]. Detailed crystallographic data for the structural analyses have been deposited with the Cambridge Crystallographic Data Centre, CCDC with deposition number 848120. Copies of this information can be obtained from The Cambridge Crystallographic Data Centre, 12 Union Road Cambridge CB21EZ, UK (fax: +44 1223 336033; e-mail: deposit@ccdc.cam.ac.uk or www: <http://www.ccdc.cam.ac.uk>). The thermogravimetric analyses were carried out at a heating rate of 20 C/min under nitrogen atmosphere using alumina powder as reference over a temperature range of 0-1400 C using a Netzsch STA 409 PC/PG thermal analyzer.

### 2.2. Synthesis of N-(2,4-dichlorobenzylidene)-3-methylbenzenamine

2,4-dichlorobenzaldehyde (175.01 mg, 1 mmol) was dissolved in absolute ethanol (50 ml) and the temperature was raised to 60°C and stirring was continued at this temperature until the aldehyde dissolved. Then 3-methylaniline (107.17 mg, 1 mmol) was added to the mixture. The whole mixture was stirred around an hour at room temperature to give a clear orange solution. Suitable crystals of the title compound for X-ray study were formed by slow evaporation of the solvent over two days at room temperature.

## 3. RESULTS AND DISCUSSIONS

The preparation of  $\text{H}_2\text{Pc}$  **2** and  $\text{CoPc}$  **3**,  $\text{CuPc}$  **4**,  $\text{NiPc}$  **5** and  $\text{ZnPc}$  **6** are shown in **Figure 1**. The structures of new compounds were characterized by using spectroscopic data and elemental analysis.

### 3.1. Structural Property of L6

The title compound **L6** was obtained by the reaction of 2,4-dichlorobenzaldehyde with 3-methylaniline in 84 % yield in ethanol solution. **L6** is a bottle straw yellow crystallite stable in air at room temperature. It is stable in air in the solid state. The crystal data and experimental details are listed in Table 1. The title compound crystallizes in the monoclinic system with space group of  $P2(1)/c$ . The molecular structure of **L6** with the atom numbering scheme and packing diagram of **L6** with inter molecular interaction along b axis are given Figure 1 (a) and (b). SEM micrograph of **L6** was investigated using a ZEISS EVO-50VP scanning electron microscope (SEM). The SEM micrograph of **L6** is shown in Figure 1 (c).



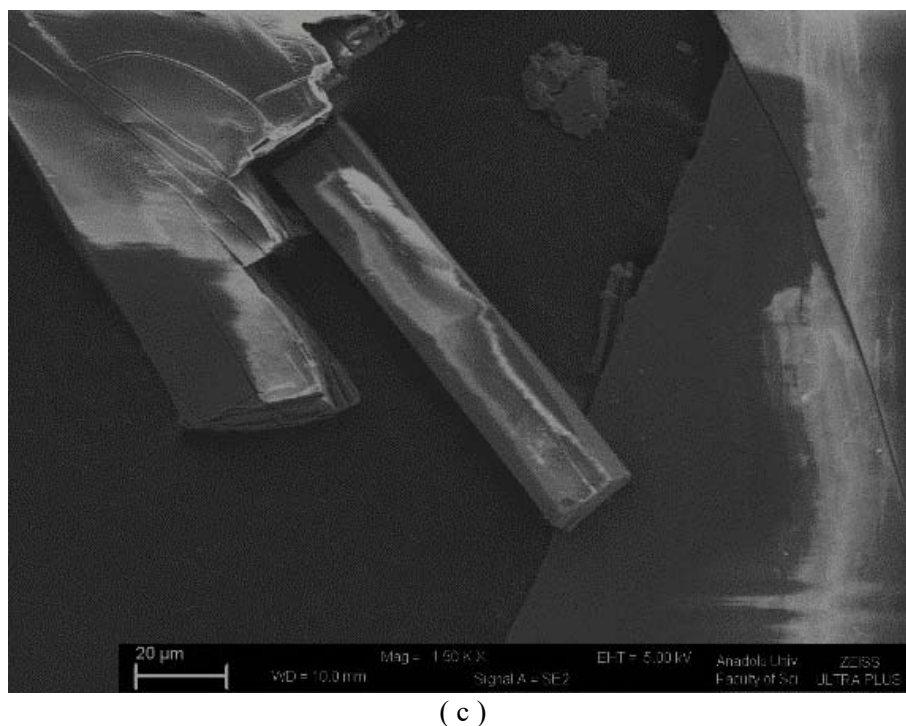


**Figure 1.** (a) The molecular structure of **L6**, (b) Packing diagram of **L6** with inter molecular interaction along b axis, (c) SEM image of **L6**

### 3.2. Computational Details

All the theoretical calculations of the title compound were carried out with the aid of the CS ChemOffice Ultra 14.0.0.117 Version for Microsoft Windows [13], Gaussian 09 program [14] and GaussView 5.0.8 [15] was used for the molecular structure optimization and computation of vibrational wavenumbers. The optimized structural parameters of the title compound were used for harmonic vibrational frequency calculations at DFT level to characterize all stationary points as minima resulting in IR intensities and Raman depolarization ratios. In order to get the more stable conformers of the title compound the potential energy surfaces (PES) as a function of the selected torsion angle were obtained. Therefore, PES were determined by using Becke's three-parameter exchange functional [16] in combination with the Lee–Yang–Parr correlation functional [17] (B3LYP) density functional theory (DFT) method with split-valance polarized 6-311++G(d,p) basis set as implemented in Gaussian 09 program package. Different possible conformers could be proposed for **L6** compound. All conformers initially were examined 6-31G(d) basis set and stability of the each conformers were also tested with 6-311++G(d,p) basis set at same theory level by using the Gaussian09 program package on a personal computer [14, 15]. As a result of computations, four conformers were obtained. Conformational energies of the title compound were calculated as a one-dimensional scan by varying the N1–C5–C6–C7 torsion angle from 0° to 360° in steps of 10°. The resulting plot of the potential energy surface (PES) scan for **L6** is shown in Figure 2.

The more favorable conformers of the title compound were selected. For the selected conformers, we started by optimizing the molecular structures in the gas phase using density functional approach. The minimum energy conformer was further optimized at B3LYP/6-311++G(d,p) basis set. The vibrational frequency calculations were performed at the same level. The fundamental normal modes were assigned. The potential energy distribution (PED) calculations were carried out by the VEDA 4 (Vibrational Energy Distribution Analysis) program on a personal computer [18]. The calculated

frequencies were scaled by 0.958 for greater than  $1700\text{ cm}^{-1}$ , 0.983 up to  $1700\text{ cm}^{-1}$  [19]. The computed frequencies were scaled factors in order to improve the agreement with the experimental results. Although accurate vibrational frequencies are more difficult to compute, it is well known that DFT calculations give excellent agreement between molecular structure parameters and experimental vibrational frequencies are scaled to compensate the approximate treatment of electron correlation, basis set deficiencies and anharmonicity [20, 21]. The scaling factors were not applied to the IR and Raman intensities. The  $^{13}\text{C}$  NMR chemical shifts of the title compound were calculated using the keyword NMR in the DFT calculation at the B3LYP level with 6-311++G(d,p) basis set.

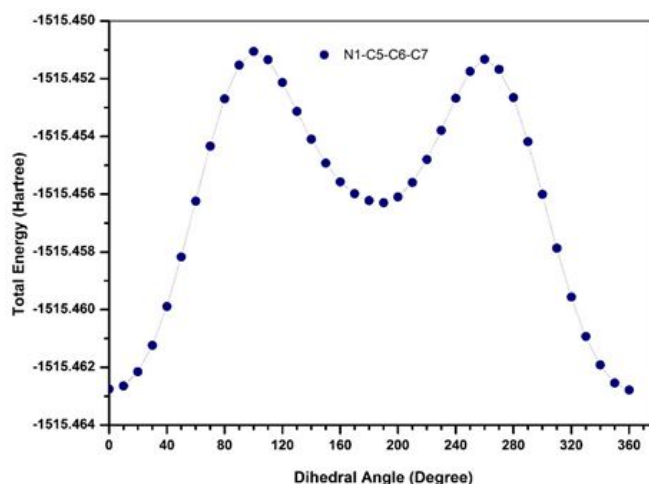


**Figure 2.** PES scan for the selected degree, T(N-C-C-C) torsional freedom

The more favorable conformers of the title compound were selected. For the selected conformers, we started by optimizing the molecular structures in the gas phase using density functional approach. The minimum energy conformer was further optimized at B3LYP/6-311++G(d,p) basis set. The vibrational frequency calculations were performed at the same level. The fundamental normal modes were assigned. The potential energy distribution (PED) calculations were carried out by the VEDA 4 (Vibrational Energy Distribution Analysis) program on a personal computer [18]. The calculated frequencies were scaled by 0.958 for greater than  $1700\text{ cm}^{-1}$ , 0.983 up to  $1700\text{ cm}^{-1}$  [19]. The computed frequencies were scaled factors in order to improve the agreement with the experimental results. Although accurate vibrational frequencies are more difficult to compute, it is well known that DFT calculations give excellent agreement between molecular structure parameters and experimental vibrational frequencies are scaled to compensate the approximate treatment of electron correlation, basis set deficiencies and anharmonicity [20, 21]. The scaling factors were not applied to the IR and Raman intensities. The  $^{13}\text{C}$  NMR chemical shifts of the title compound were calculated using the keyword NMR in the DFT calculation at the B3LYP level with 6-311++G(d,p) basis set.

### 3.3. Molecular Geometry

In the gas phase the selected molecular properties of the possible conformers of the compound **L6** within calculated B3LYP theory level with 6-311 G ++ (d, p) basis sets are given Table 2. The Table 2 point out that the C2 is a more stable conformer at room temperature (298 K) among the others taking into account the energies along with the population factors values. It is also worth noticing that the various basis sizes effect on  $\Delta\text{SCF}$  (self-consistent field energy) and  $\Delta\text{G}$  (the change in free energy) energies are not great and that the stability order for the conformers remains the same with the basis sets. The conformers are also in agreement with the single crystal structure data. In consistence with results obtained in the solid state, theoretical calculations predict that in the gas phase conformer C2 is the most stable ones. In addition, based on the theoretical results a planar structure for the conformers was found.

**Table 2.** The selected molecular properties of the possible conformers of **L6** molecule within calculated B3LYP theory level with 6-311++G(d,p) basis set

Molecular Properties (B3LYP/6311++G(d,p))	Possible conformers			
	L61	L62	L63	L64
Symmetry	C <sub>1</sub>	C <sub>1</sub>	C <sub>1</sub>	C <sub>1</sub>
$\mu_{\text{total}}$ (debye)	1.29150	1.29270	2.41600	2.78380
$E_{\text{total}}$ (kcal/mol)	-950967.96560	-950968.01960	-950963.98410	-950963.856010
$\Delta E_0$ (kcal/mol)	0.05400	0	4.03550	4.16350
$\Delta G$ (kcal/mol)	-950863.8410	-950864.72080	-950860.74300	-950860.67900
$\delta\Delta G$ (kcal/mol)	0.87980	0	3.97780	4.04180
HOMO (eV)	-0.30607	-0.30606	-0.30641	-0.30651
LUMO (eV)	-0.21705	-0.21697	-0.21237	-0.21226
$\Delta L-H$ (eV)	0.08902	0.08909	0.09403	0.09425
$N_i$	39.75000	56.77000	1.79000	1.73000

The corresponding some structural parameters such as bond lengths, bond angles and dihedral angles optimized and experimental of the possible conformers of the compound **L6** in the gas phase obtained at the B3LYP theory level with 6311G++ (d, p) basis set are given Table 3. To the best of our knowledge, experimental data on the geometric structure of **L6** molecule is not available in the literature. Other bond length (C=N) in the **L6** molecule that is calculated 1.277 Å and measured 1.276 Å. These values are also consistent with the similar studies [22-26]. The changes in the bond length of the C–H bond on substitution may be due to a change in the charge distribution on the carbon atom of the benzene ring [27-31]. The C–Cl bond lengths (1.738 and 1.741 Å) are in good agreement with the mean value (1.741 ± 0.016 Å) [25]. The optimized bond lengths of C–H and C–Cl for B3LYP with 6-311++G(d,p) method were also in good agreement for similar molecules [27, 28, 30, 32].

**Table 3.** The selected bond lengths (Å), angles (°) and torsion angles (°) optimized and experimental of the possible conformers **L6** molecule within calculated B3LYP theory level with 6-311++G(d,p) basis set

Coordinate <sup>a</sup>	DFT/6-311++G(d,p)				
	L6-1	L6-2	L6-3	L6-4	Experimental
<b>Bond lengths (Å)</b>					
C11–C9	1.753	1.753	1.753	1.753	1.738
C12–C10	1.762	1.761	1.747	1.747	1.741
N1–C4	1.401	1.407	1.406	1.406	1.423
N1–C5	1.277	1.277	1.274	1.274	1.276
C3–C4	1.400	1.402	1.402	1.403	1.397
C4–C12	1.400	1.402	1.402	1.402	1.398
C5–H5	1.093	1.093	1.099	1.099	0.950
C5–C6	1.471	1.470	1.470	1.470	1.473
C6–C7	1.406	1.406	1.407	1.403	1.402
C6–C10	1.404	1.404	1.410	1.410	1.398
<b>Angles (°)</b>					
C4–N1–C5	120.2	120.2	119.9	119.8	119.8
N1–C4–C3	122.9	117.5	117.5	122.8	115.6
N1–C4–C12	117.8	123.2	123.1	117.9	124.8
N1–C5–H5	121.9	122.0	121.0	120.9	119.8
N1–C5–C6	121.4	121.4	125.7	125.8	120.3
H5–C5–C6	116.6	116.6	113.3	113.2	119.9
C6–C7–H7	117.4	117.4	118.1	118.1	119.0
C12–C10–C6	121.2	121.2	122.8	122.8	120.3
C4–C12–H12	118.9	120.1	120.0	118.9	120.3

Torsion angles (°)					
C4–N1–C5–H5	-3.8	3.8	-3.9	4.0	-0.0
C4–N1–C5–C6	177.1	-177.1	177.8	-177.7	179.9
H3–C3–C4–N1	-1.1	-0.8	-0.7	1.02	-0.6
N1–C4–C12–H12	-0.8	1.0	-1.1	0.8	-0.5
N1–C5–C6–C7	-1.9	1.7	173.2	-173.7	-17.8
N1–C5–C6–C10	178.1	-178.4	-6.8	6.3	163.0
C5–C6–C7–H7	0.0	0.0	0.3	-0.1	1.5
C5–C6–C10–C12	-0.1	0.0	-1.1	0.9	-2.8

In general, calculated geometric parameters are in good agreement with those obtained from experimental results. Generally, from the theoretical values, it is found that most of the optimized bond distances are slightly longer than the experimental distances. The small differences may be due to that the theoretical calculations belong to isolates molecules in gaseous phase without any intermolecular interactions and the experimental results belong to molecules in solid state.

### 3.4. Electronic Spectra

The highest occupied molecular orbitals (HOMO) and the lowest unoccupied molecular orbitals (LUMO) are called as frontier molecular orbitals (FMOs). HOMO (H) and LUMO (L) are the most important orbitals in molecules and the energy gap between HOMO and LUMO is a useful parameter in determining the optical and electrical properties. Based on the optimized structure, the surfaces of HOMO and LUMO calculated using DFT method at B3LYP/6-311++G(d, p) base set in gaseous phase were given in Figure 3. In Figure 3, the positive and negative phase were represented in red and green color, respectively. The energies of HOMO and LUMO orbitals of the title compound in gas phase are -0.30606, -0.21697 eV respectively. The HOMO and LUMO orbital energy gap is equal (energy gap=LUMO-HOMO) +0.08909 eV and explains the possible charge transfer interactions taking place within the molecule.

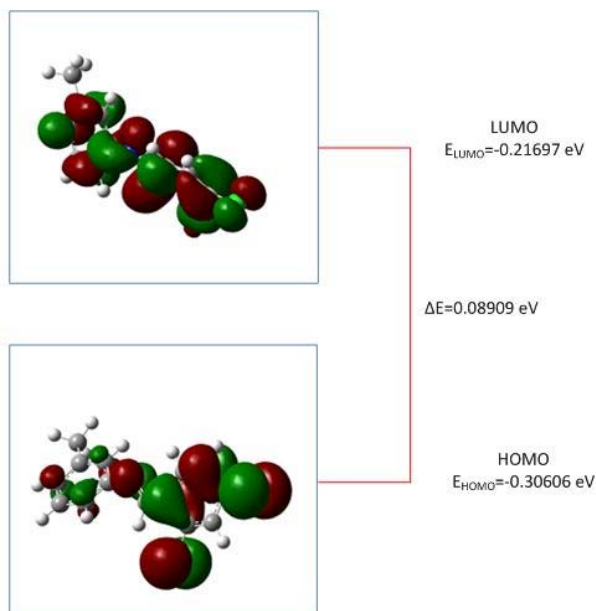


**Figure 3.** Highest occupied and lowest unoccupied orbitals of **L6**

The UV-Vis spectrum provide the most detailed information about the electronic structure of a compound. The UV-Vis spectrum of the ligand was recorded in ethanol at room temperature. The experimental and theoretical UV-Vis spectra of **L6** in ethanol solvent are given in Figure 4 (a) and (b). Generally, in the electronic absorption spectra of Schiff base compounds the bands (300-400 nm)

show azomethine C=N group. The first bands at higher energy (200-300 nm) are attributed to  $\pi - \pi^*$  transitions associated with the phenyl ring and the second bands at lower energy are related to  $\pi - \pi^*$  transitions associated with the azomethine group. In the molecule, the band in the region 300-400 nm is attributed to the  $n - \pi^*$  transition. The calculated absorption wavelengths ( $\lambda_{\max}$ ) are in good agreement with the experimental values. These values are similar to those found in related Schiff base compounds [2, 4].

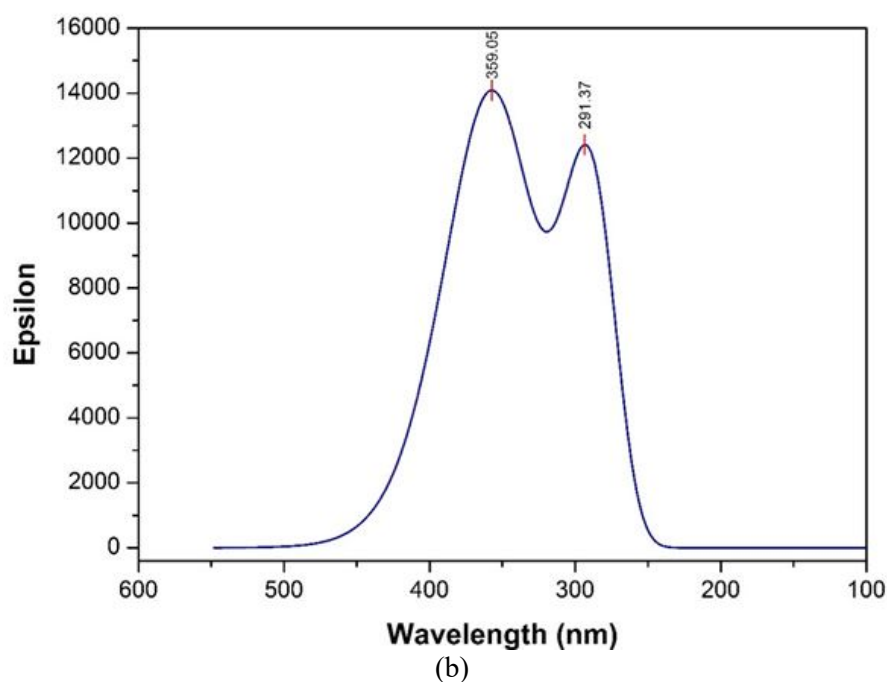
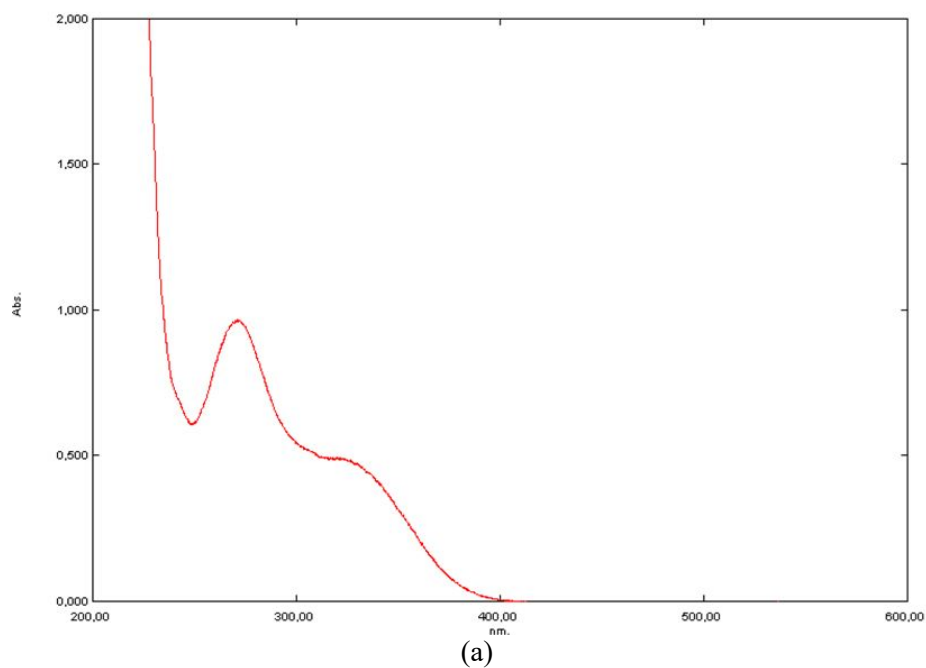


**Figure 4 (a)** The experimental and **(b)** theoretical UV-Vis spectra of **L6** in ethanol solvent

### 3.5. Vibrational Spectral Analysis

To the best of our knowledge, there is no detailed quantum chemical study for the molecular structure and vibrational spectra of **L6** molecule. The assignments of the normal vibrational modes of the most stable conformer of investigated compound along with the observed fundamentals, unscaled frequencies obtained by B3LYP/6-311++G(d,p) calculations and scaled frequencies as well as the PED descriptions are given in Table 4. The experimental and theoretical infrared and Raman spectra of **L6** compound were presented in Figure 5 and 6 for comparative purposes. The **L6** molecule consist of 28 atoms, which have 78 normal modes of fundamental vibrations and it belongs to C1 symmetry group. In order to simplify the experimental assignment as much as possible, it is necessary to clarify characteristic group vibrations.

The aromatic structure shows the presence of C–H stretching vibrations in the region 3000-3100  $\text{cm}^{-1}$  which is the characteristic region for ready identification of C–H stretching vibrations [33-35]. Accordingly, in the present study the FT-IR bands at 3058, 3026  $\text{cm}^{-1}$  and Raman bands at 3099, 3073  $\text{cm}^{-1}$  are assigned to the C–H stretching vibrations of the title compound. The bands at 2994, 2940, 2918 and 2859  $\text{cm}^{-1}$  in FT-IR spectrum and 2928  $\text{cm}^{-1}$  in Raman spectrum are attributed to the C–H stretching vibrations. The corresponding scaled calculated frequencies of CH stretching vibrations at 2973, 2948, 2946 and 2896  $\text{cm}^{-1}$  are good agreement with the experimental data. The CH in-plane bending vibrations, the vibrational bands of the sample were observed at 1170, 1146, 1135 and 1098  $\text{cm}^{-1}$  in infrared spectrum and 1066, 1011  $\text{cm}^{-1}$  in Raman spectrum. The CH out-of-plane deformation vibrations of **L6** were recorded at 972, 963, 953, 927, 896, 868 and 763  $\text{cm}^{-1}$  in infrared spectrum and 885  $\text{cm}^{-1}$  in Raman spectrum. The characteristic band of **L6** compound which contain azomethine group was observed at 1598 and 1610  $\text{cm}^{-1}$  in the FT-IR and Raman spectrum respectively. The vibrational spectra of the compound also showed several bands corresponding to aromatic CC stretching, HCC and HCN bending and some torsion bands. The vibrations belonging to the bond between the ring and the halogen atoms are also observed below 900  $\text{cm}^{-1}$ . Ring stretching and CH bending modes show the 1500-1000  $\text{cm}^{-1}$  region of the Raman spectrum. The above conclusions are in very good agreement with literature values [19, 24, 26, 27, 30, 33, 36-40].

**Table 4** The vibrational wavenumbers ( $\text{cm}^{-1}$ ) of L6

Mode	Experimental		B3LYP/6-311++G(d,p)				P.E.D.s $\geq$ 5
	IR (Nujol)	Raman (solid)	$\nu^b$	$\nu^c$	$I_{\text{IR}}^d$	$I_{\text{R}}^d$	
1	3058 w	3099 vw	3172	3039	19.05	127.13	vCH(90)
2	3026 vw	3073 w	3158	3025	3.64	73.17	vCH(96)
3	2994 vw	-	3103	2973	15.68	72.61	vCH(99)
4	2940 vw	-	3077	2948	17.81	106.04	vCH(97)
5	2918 w	-	3075	2946	23.03	26.86	vCH(96)
6	2859 vw	2928 w	3023	2896	34.22	315.37	vCH(100)
7	1598 m	1610 s	1677	1649	35.31	2409.10	vCN(67)
8	1583 s	-	1637	1609	43.20	617.65	vCC(41)
9	-	1582 vs	1619	1592	106.07	1708.94	vCC(24)
10	1553 m	-	1607	1580	56.69	2424.21	vCC(43) + $\delta$ HCC(12)
11	1519 vw	-	1583	1556	22.84	205.54	vCC(50) + $\delta$ HCC(10)
12	1471 s	1484 vw	1514	1488	51.45	76.60	$\delta$ HCC(48)
13	-	1436 vw	1495	1470	30.70	148.42	$\delta$ HCC(41) + $\delta$ HCH(23)
14	1417 vw	-	1490	1465	7.75	11.20	$\delta$ HCH(78) + $\tau$ HCCC(11)
15	1385 s	1395 w	1454	1429	2.68	90.58	vCC(30)
16	1371 vw	1376 w	1415	1391	1.26	38.01	$\delta$ HCH(91)
17	1361 s	-	1412	1388	26.04	394.85	vCC(33) + $\delta$ HCC(29)
18	1328 vw	-	1397	1373	22.35	67.15	$\delta$ HCN(60)
19	1284 vw	1301 w	1341	1318	1.79	13.89	vCC(37) + $\delta$ HCC(50)
20	1272 w	1258 m	1316	1294	4.42	137.85	vCC(23)
21	1261 w	-	1303	1281	1.57	5.39	vCC(39)
22	1245 w	1255 m	1288	1266	9.50	121.86	vCC(14) + $\delta$ HCC(41)
23	1209 w	1150 s	1271	1249	13.01	701.49	vCN(15) + vCC(12) + $\delta$ HCC(13)
24	1170 vw	-	1229	1208	9.61	543.12	vCC(35) + $\delta$ HCC(15)
25	1146 w	-	1192	1172	0.12	18.99	$\delta$ HCC(73) + vCC(14)
26	1135 m	1066 vw	1171	1151	2.80	149.16	vCN(15) + vCC(11) + $\delta$ HCC(29)
27	1098 s	1011 w	1149	1130	34.96	580.16	vCC(12) + $\delta$ HCC(38)
28	1050 s	940 vw	1110	1091	68.39	72.86	vCC(53) + vCIC(12)
29	1000 w	-	1062	1044	23.27	2.27	$\delta$ CCC(32) + $\tau$ HCCC(16)
30	972 m	885 vw	1021	1004	6.48	21.44	$\tau$ HCCC(42)
31	963 vw	-	1015	998	1.40	42.14	$\delta$ CCC(53) + $\tau$ HCNC(15)
32	953 m	-	1005	989	5.53	151.98	$\tau$ HCNC(41) + $\tau$ HCCC(14)
33	927 w	-	947	931	17.54	47.63	$\delta$ CCC(24) + vCN(15) + vCC(13)
34	896 s	-	918	902	7.88	1.47	$\tau$ HCCC(72)
35	868 vs	-	879	864	41.34	29.69	$\delta$ CCC(38)
36	825 vs	-	843	829	23.58	1.93	$\tau$ HCCC(74)
37	794 m	-	805	791	22.10	13.36	$\tau$ HCCC(26) + vCIC(10)
38	769 vs	-	787	774	40.56	7.64	$\tau$ HCCC(49)
39	763 vs	742 vw	738	725	18.23	7.54	vCC(12) + $\delta$ CCC(12)
40	731 m	-	728	716	3.03	1.72	$\tau$ CCCC(68)
41	707 vs	-	706	694	16.74	0.78	$\tau$ HCCC(25) + $\tau$ CCCC(27)
42	682 vs	680 w	676	665	1.00	21.16	$\delta$ CCC(54) + vCC(12)
43	609 m	624 vw	618	607	4.09	5.29	vCC(14) + vCIC(15) + $\delta$ CCC(23)
44	576 m	-	596	586	2.34	8.87	$\tau$ CCCC(12) + $\tau$ NCCC(12)
45	554 w	-	573	563	4.90	0.62	$\tau$ HCCC(14) + $\tau$ CCCC(14) + $\tau$ CICCC(25)
46	545 m	531 w	529	520	0.34	6.32	$\delta$ CCC(29) + vCC(12)
47	516 w	-	520	511	2.80	6.63	$\delta$ CCC(26) + $\delta$ NCC(18)
48	461 w	-	472	464	7.99	1.18	$\tau$ CCCC(37) + $\tau$ CICCC(12)
49	445 s	465 vw	451	443	12.19	12.68	$\tau$ CCCC(16) + $\tau$ CCCC(12)
50	438 w	-	448	440	5.10	0.12	$\tau$ CCCC(15)
51	408 w	429 vw	418	411	9.21	13.38	vCIC(30) + $\delta$ CCC(10)

<sup>a</sup>vs: very strong, s: strong, m: medium, w: weak, vw: very weak, br: broad, sh: shoulder.  $\nu$ ,  $\delta$  and  $\tau$  denote stretching, bending and torsion modes, respectively.

<sup>b</sup>Unscaled values

<sup>c</sup>Scaled values. Scaled with 0.958 above 1700  $\text{cm}^{-1}$ , 0.983 under 1700  $\text{cm}^{-1}$ .

<sup>d</sup> $I_{\text{IR}}$  and  $I_{\text{R}}$ : calculated infrared intensities and Raman activities. PED data are taken from VEDA4 [26].

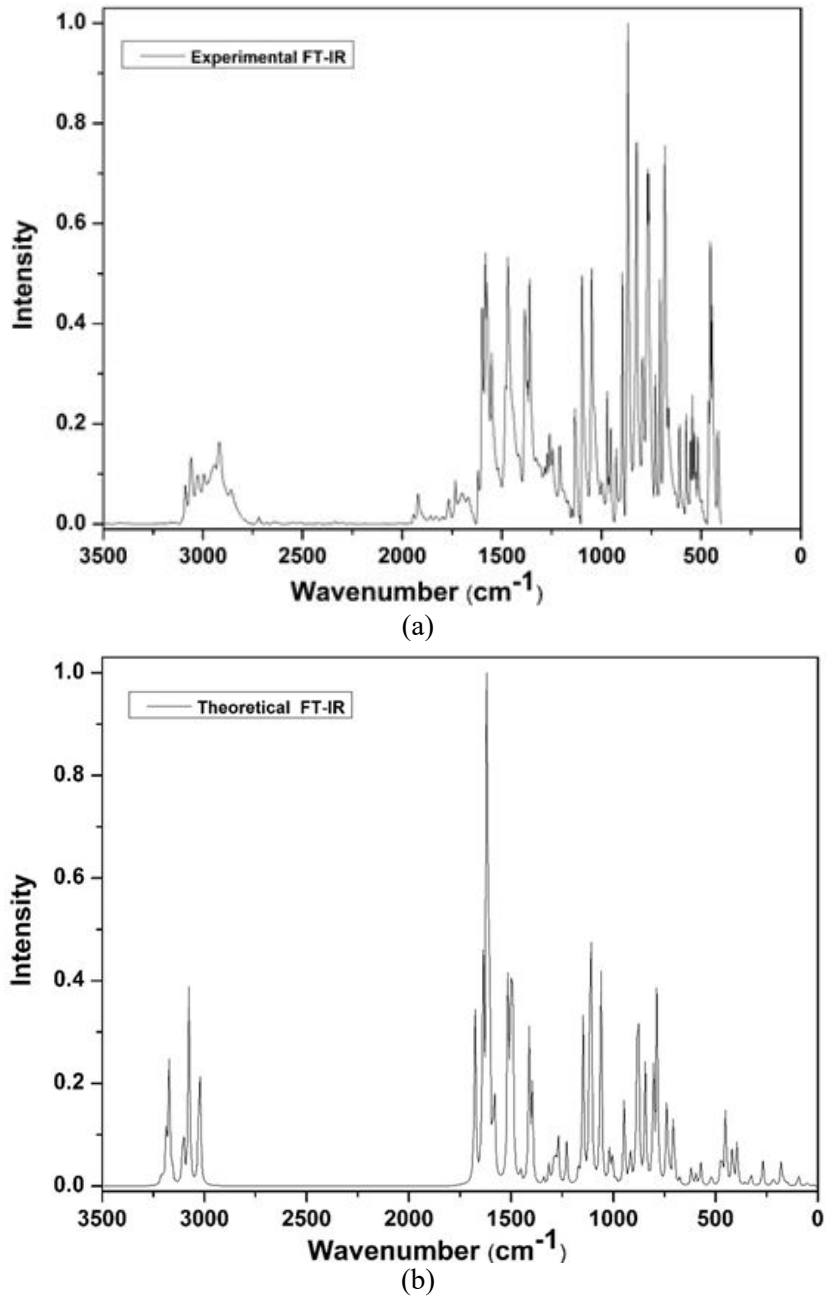
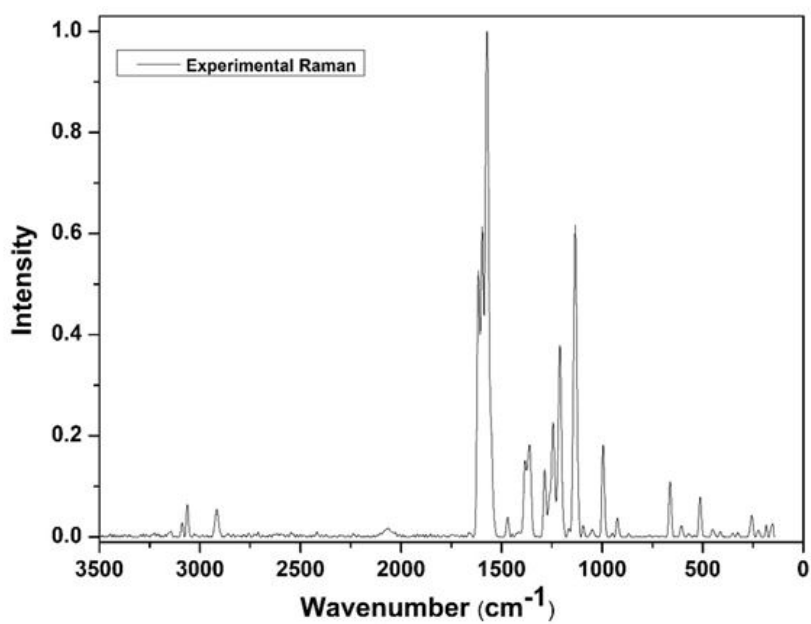
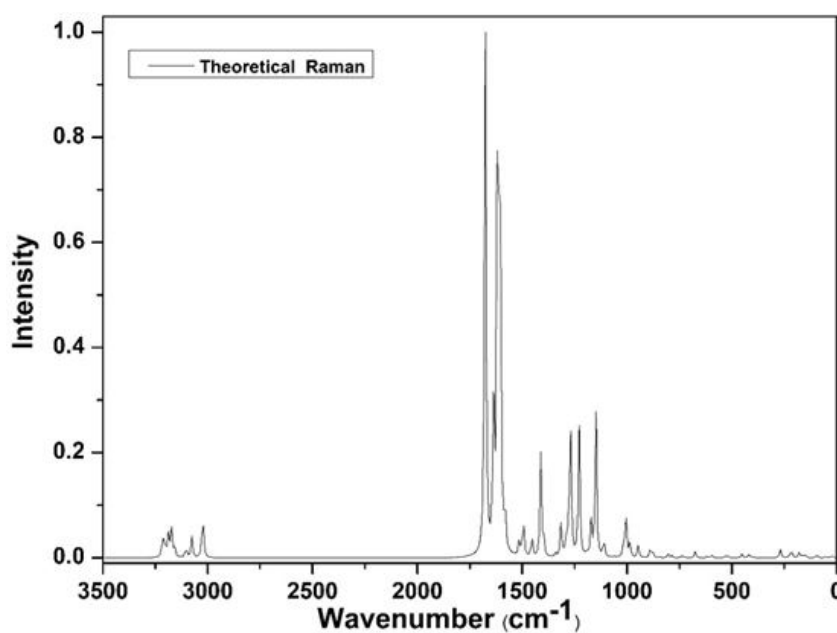


Figure 5 (a) Experimental and (b) theoretical infrared spectra of L6



(a)



(b)

**Figure 6** Experimental (a) and theoretical (b) Raman spectra of L6

The correlation between the experimental and calculated wavenumbers can be seen by plotting the calculated versus experimental wavenumbers (for infrared and Raman). The correlation graphics were plotted in Figure 7 (a) and (b) for infrared and Raman, respectively, based on the DFT/B3LYP method. As can be seen from Figure 7, the relations are usually linear and described by Equations 1 and 2:

$$v_{\text{cal.}} = 0.9797v_{\text{exp.}} + 36.875 \quad (R^2 = 0.9964 \text{ for infrared}) \quad (1)$$

$$v_{\text{cal.}} = 1.0038v_{\text{exp.}} + 6.3857 \quad (R^2 = 0.9994 \text{ for Raman}) \quad (2)$$

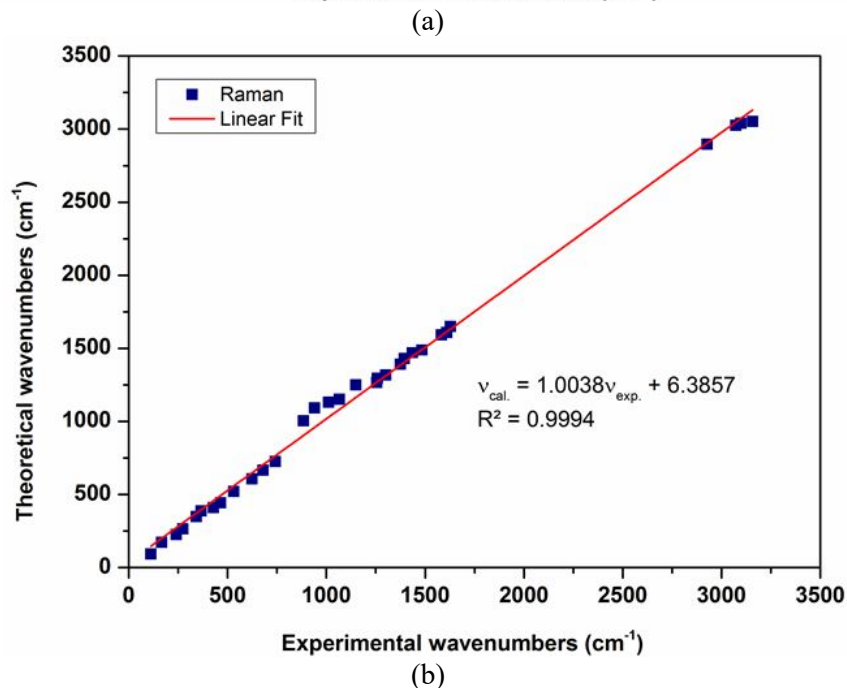
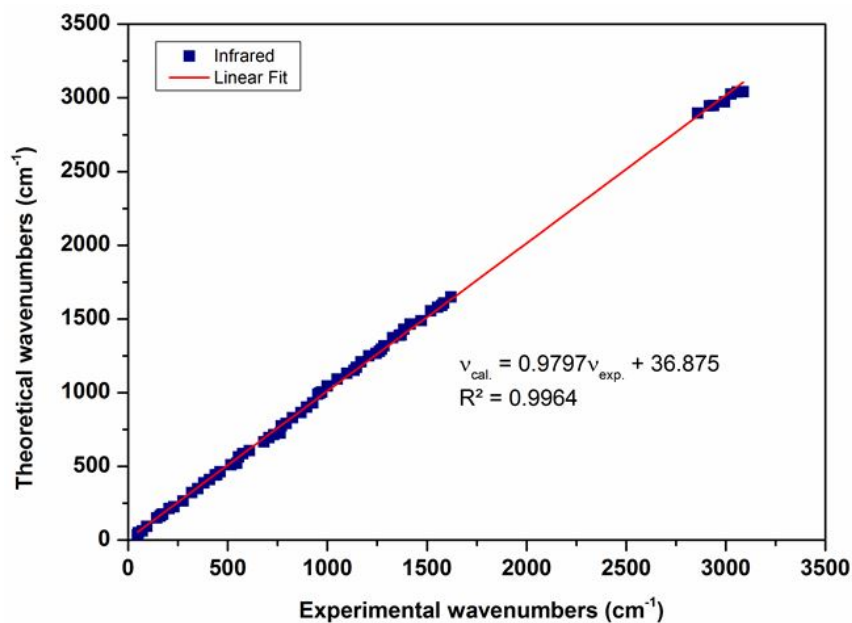


**Figure 7** The correlation graphics of experimental (a) and calculated (b) wavenumbers of L6

### 3.6. <sup>1</sup>H and <sup>13</sup>C NMR Chemical Shift Assignment

The experimental and theoretical <sup>1</sup>H and <sup>13</sup>C NMR spectra of the title compound are shown in Figure 8 and Figure 9, respectively. <sup>13</sup>C NMR spectrum of the compound exhibited characteristic peak in the region 21.69 ppm assignable to the methylene groups and singlets over the range 121.70- 160.24 ppm characteristic of the aromatic groups. Aromatic ring protons (in the region *ca.* 7.19 and 9.10 ppm),

methyl protons (at *ca.* 2.36 ppm) and methylene protons (in the region 2.7-3.5 ppm) in proton NMR, clearly indicating the aromatic and methyl hydrogens. Table 5 and 6 shows the  $^{13}\text{C}$  and  $^1\text{H}$  NMR chemical shifts (ppm) for the compound.

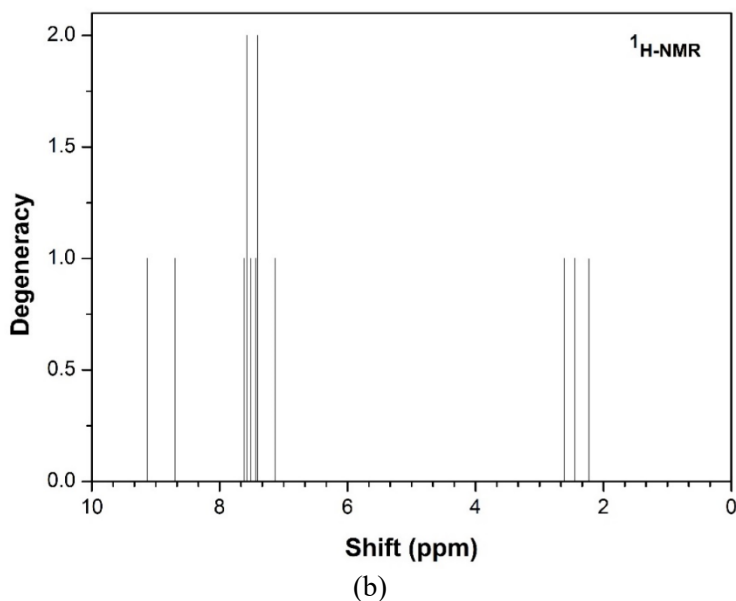
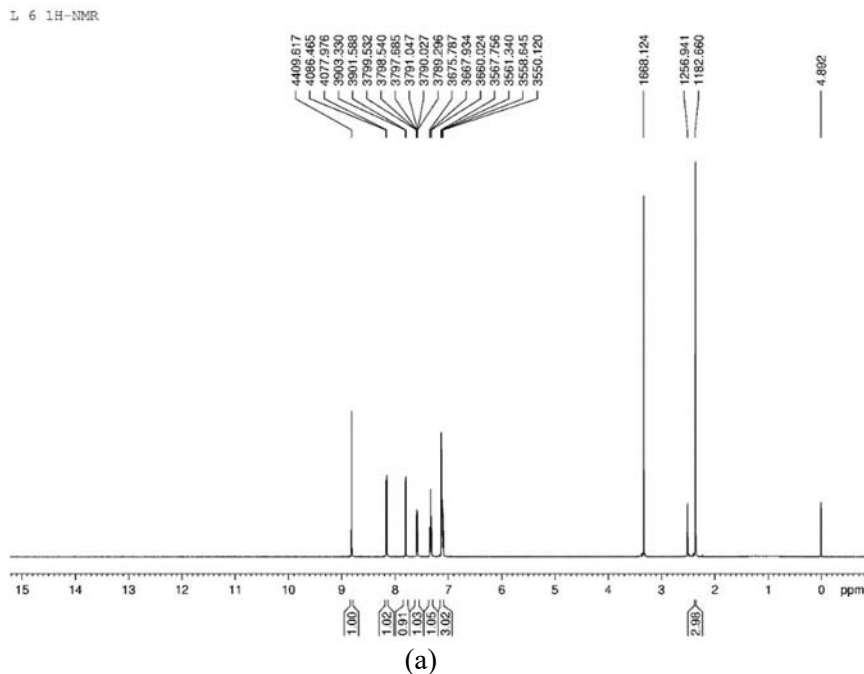


**Figure 8 (a)** Experimental and **(b)** theoretical  $^1\text{H}$ -NMR spectra of **L6**

The theoretical  $^1\text{H}$  and  $^{13}\text{C}$  NMR chemical shifts at the B3LYP/6-311++G(d,p) levels of theory along with experimental data are given in Table 5 and Table 6, respectively. As can be seen, the theoretical results are in very good agreement with the experimental data. Compared with the experimental  $^1\text{H}$  NMR chemical shifts, correlation graphic based on the theoretical shifts is presented in Figure 10. The correlation graphic between experimental and calculated  $^{13}\text{C}$  NMR chemical shift is shown in Figure 11. The  $^1\text{H}$  and  $^{13}\text{C}$  NMR chemical shifts correlation values are 0.9893 and 0.9856, respectively.

**Table 5** Theoretical and experimental  $^1\text{H}$  NMR chemical shifts (all values in ppm) of L6

Experimental	DFT/B3LYP	Assignment
9.104	8.82	21-H
8.683	8.17	19-H
7.6263	7.81	18-H
7.5541	7.60	20-H
7.5071	7.35	23-H
7.3952	7.33	24-H
7.3518	7.31	22-H
7.1976	7.13	25-H
2.3671	2.37	26-H, 27-H, 28H

**Table 6** Theoretical and experimental  $^{13}\text{C}$  NMR chemical shifts (all values in ppm) of L6

Experimental	DFT/B3LYP	Assignment
160.2431	155.5	7-C
159.0383	151.34	9-C
151.6762	139.25	13-C
151.0816	137.14	4-C
147.3748	136.21	11-C
147.3748	132.18	3-C
134.8123	130.14	5-C
134.3862	130.10	1-C
133.5209	130.04	12-C
132.5112	129.64	2-C
132.1146	128.54	6-C
126.9945	127.92	14-C
121.7082	118.76	10-C
21.6964	21.41	15-C

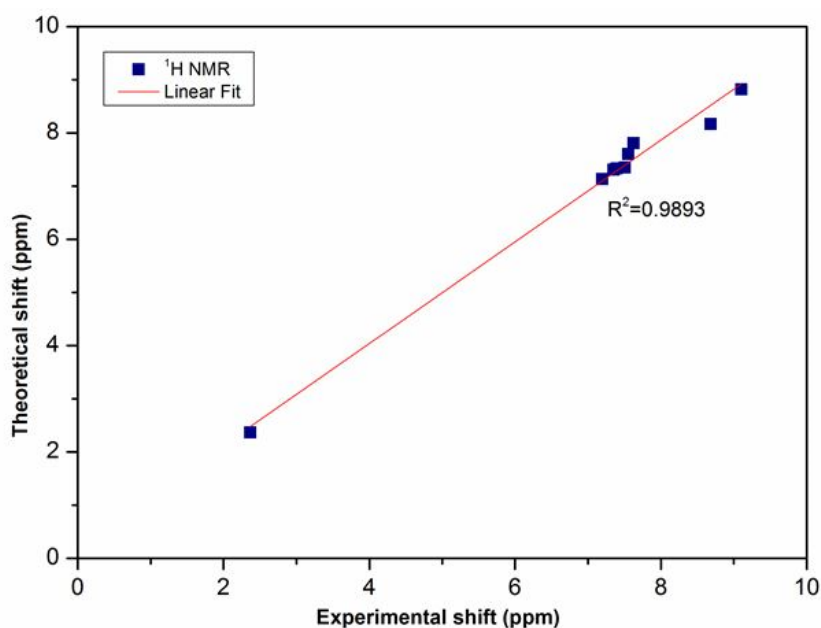


**Figure 10** The correlation graph of experimental and calculated  $^1\text{H}$  NMR chemical shifts of L6

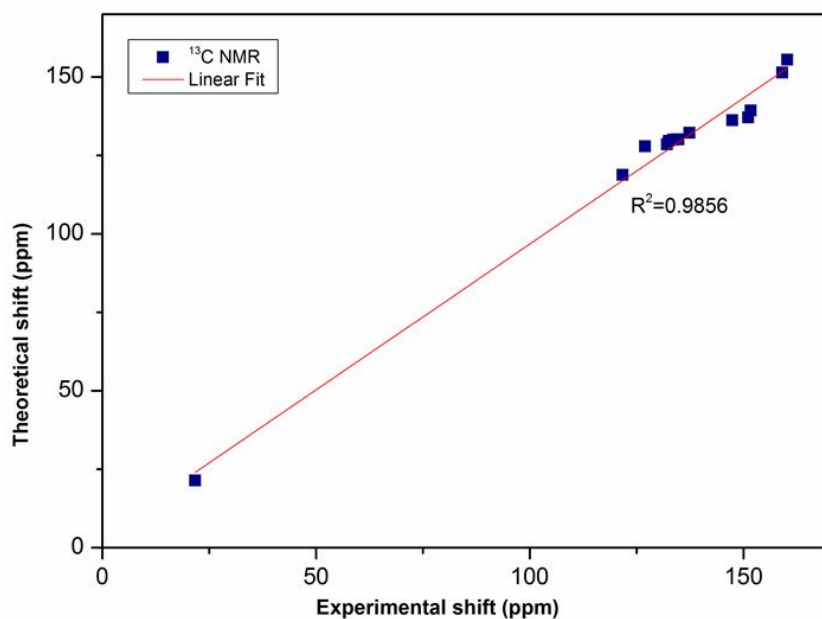


**Figure 11** The correlation graph of experimental and calculated  $^{13}\text{C}$  NMR chemical shifts of L6

### 3.7. Thermal Analysis

The thermal stability of the title was analyzed by thermogravimetric analysis (TGA). The weight loss profiles are analyzed by the amount or percent of weight loss at any given temperature. Thermogravimetric analysis (TGA) and differential thermal analysis (DTA) curves of L are presented in Figure 12. The TGA curve of L displays four stages of mass loss within the temperature range of 0-1400 °C. The TG curve of ligand L6, refers to two stages of mass losses at temperature ranges from 0 to 400 °C. These stages involved mass losses of 100.0% (found 100.51%) for the first and second steps of decomposition, respectively. These mass losses may be due to the successive losses of  $\text{C}_{14}\text{H}_{11}\text{Cl}_2\text{N}$  molecule as gases at the given temperature range [41].

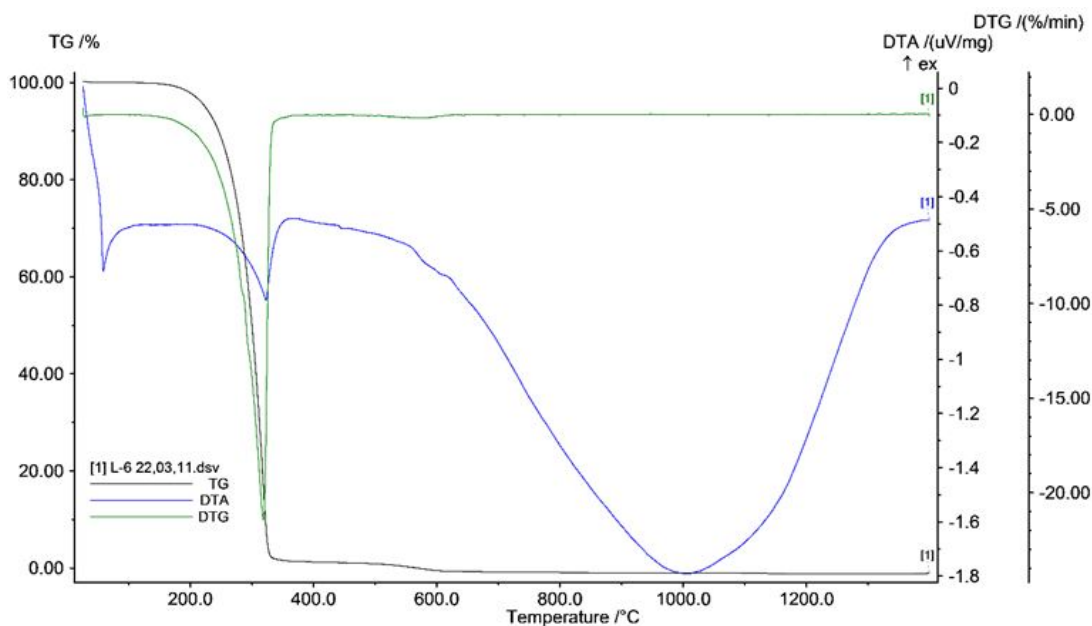


**Figure 12** TGA/DTA/DTG curve of ligand L6

#### 4. CONCLUSIONS

The Schiff-base compound **L6** was synthesized and the structure of **L6** was confirmed by spectroscopic (FT-IR, Raman,  $^1\text{H}$  NMR,  $^{13}\text{C}$  NMR, UV-VIS, single crystal X-ray diffraction) and thermal techniques. The vibrational wavenumbers were examined theoretically using quantum chemical computations and the normal modes were assigned by potential energy distribution calculation. The HOMO and LUMO analysis was used to determine the charge transfer within the molecule. The  $^1\text{H}$  and  $^{13}\text{C}$  NMR chemical shifts of **L6** compound was analyzed. The geometrical parameters of the title compound are in good agreement with single crystal X-ray results. Crystallographic data for the title compound have been deposited with the Cambridge Crystallographic Data Centre, CCDC reference number 848120 The characteristic double bond C=O shows vibrational absorption around  $1700\text{ cm}^{-1}$ , but there was no identification for the free carbonyl group in the title compound. On the basis of this, one can conclude that this compound is mainly existed in Schiff base form, in agreement with the conclusion which was obtained from NMR and Raman studies. Detailed vibrational assignments of the compound was ascribed to its structural vibrations. The assignments of fundamental frequencies were confirmed by the agreement between the calculated and experimental results. Comparison of the calculated vibrational spectra with the experimental data provides reliable assignments of all observed bands in FT-IR and Raman spectra of the title compound. The reasonable agreement between the theoretical and experimental data reflects to the great extent the suitability of the applied basis set, 6-311++g(d,p) for this type of work and confirms the suggested structure.

#### ACKNOWLEDGMENTS

We would like to thank the BAP of the Anadolu University (Nos. 1102F027 and 1304F064) for its financial support for Gaussian 09 and Gauss View 5.0 programs. The authors are grateful to Mustafa Çobancı, the SAM, for thermal analysis.

#### REFERENCES

- [1] Blagus A, Cinčić D, Frisčić T, Kaitner B, Stilinović V. Schiff bases derived from hydroxyaryl aldehydes: molecular and crystal structure, tautomerism, quinoid effect, coordination compounds. *Maced J Chem and Chem Eng* 2010; 29(2); 117-138.
- [2] Dueke-Eze CU, Fasina TM, Idika N. Synthesis, electronic spectra and inhibitory study of some Salicylaldehyde Schiff bases of 2-aminopyridine. *AJPAC* 2011; 5(2); 13-18.
- [3] Khaloji AD, Mighani H, Gotoh K, Ishida H. Synthesis, Characterization, Structure, Ab Initio and DFT Calculations of 2-Amino-N-(3-phenylprop-2-enylidene)aniline. *J Chem Crystallogr* 2011; 41; 1154-1157.
- [4] Pramanik HAR, Das D, Paul PC, Mondal P, Bhattacharjee CR. Newer mixed ligand Schiff base complexes from aquo-N-(2'-hydroxy acetophenone) glycinatocopper(II) as synthon: DFT, antimicrobial activity and molecular docking study. *Journal of Molecular Structure* 2014; 1059; 309-319.
- [5] Singh AK, Pandey SK, Pandey OP, Sengupta SK. Synthesis and spectral characterization of Zn(II) microsphere series for antimicrobial application. *Journal of Molecular Structure* 2014; 1074; 376-383.
- [6] Li ZZ, Gu Z, Yin K, Zhang R, Deng Q, Xiang JN. Synthesis of substituted-phenyl-1,2,4-triazol-3-thione analogues with modified d-glucopyranosyl residues and their antiproliferative activities. *Eur. J. Med. Chem.* 2009; 44; 4716-4720.

- [7] Li YG, Dong XW, Ai R, Xu XL, Zhu HL. Synthesis and Crystal Structure of a New Schiff Base Ligand and Its Cobalt(II) Complex<sup>1</sup>. Russian J Coord Chem 2011; 37; 523-527.
- [8] Khalaji AD, Chermahini AN, Fejfarova K, Dusek M. Synthesis, characterization, crystal structure, and theoretical studies on Schiff-base compound 6-[(5-Bromopyridin-2-yl)iminomethyl]phenol. Struc Chem 2010; 21; 153-157.
- [9] Magar BK, Kirdant AS, Chondhekar TK. Formation of N-salicylidene-p-methylaniline: A kinetic study. Der Chemica Sinica 2014; 5(1); 95-100.
- [10] Jadhav SM, Shelke VA, Munde AS, Shankarwar SG, Chondhekar TK. Synthesis, characterization, potentiometry, and antimicrobial studies of transition metal complexes of a tridentate ligand. J Coord Chem 2010; 63(23); 4153-4164.
- [11] Shelke VA, Jadhav SM, Shankarwar SG, Munde AS, Chondhekar TK. Synthesis and Characterization of Tetradentate N<sub>2</sub>O<sub>2</sub> Schiff Base Ligand and its Rare Earth Metal Complexes. J Korean Chem Soc 2011; 55(3); 436-443.
- [12] Patel PR, Zele S. Preparation and characterization of some lanthanide complexes involving a heterocyclicβ-diketone. Ind. Chem 1999; 38A; 563-567.
- [13] ChemBioDraw Ultra 14 Individual ASL SN Win., Download Individual Two Year Term English Windows, 2014.
- [14] Gaussian 09, Revision B.01. Frisch, M. J.; Trucks, G. W.; Schlegel, H. B.; Scuseria, G. E.; Robb, M. A.; Cheeseman, J. R.; Scalmani, G.; Barone, V.; Mennucci, B.; Petersson, G. A.; Nakatsuji, H.; Caricato, M.; Li, X.; Hratchian, H. P.; Izmaylov, A. F.; Bloino, J.; Zheng, G.; Sonnenberg, J. L.; Hada, M.; Ehara, M.; Toyota, K.; Fukuda, R.; Hasegawa, J.; Ishida, M.; Nakajima, T.; Honda, Y.; Kitao, O.; Nakai, H.; Vreven, T.; Montgomery, J. A., Jr.; Peralta, J. E.; Ogliaro, F.; Bearpark, M.; Heyd, J. J.; Brothers, E.; Kudin, K. N.; Staroverov, V. N.; Kobayashi, R.; Normand, J.; Raghavachari, K.; Rendell, A.; Burant, J. C.; Iyengar, S. S.; Tomasi, J.; Cossi, M.; Rega, N.; Millam, J. M.; Klene, M.; Knox, J. E.; Cross, J. B.; Bakken, V.; Adamo, C.; Jaramillo, J.; Gomperts, R.; Stratmann, R. E.; Yazyev, O.; Austin, A. J.; Cammi, R.; Pomelli, C.; Ochterski, J. W.; Martin, R. L.; Morokuma, K.; Zakrzewski, V. G.; Voth, G. A.; Salvador, P.; Dannenberg, J. J.; Dapprich, S.; Daniels, A. D.; Farkas, Ö.; Foresman, J. B.; Ortiz, J. V.; Cioslowski, J.; Fox, D. J. Gaussian, Inc., Wallingford CT, 2009.
- [15] Dennington RD, Keith TA, Millam JM, GaussView 5.0.8, Gaussian Inc., Wallingford CT 2008.
- [16] Becke AD. Density-functional thermochemistry. III. The role of exact Exchange, J Chem Phys 1993; 98; 5648-5652.
- [17] Lee C, Yang W, Parr RG. Development of the Colle-Salvetti correlation-energy formula into a functional of the electron density, Phys. Rev. B 1988; 37; 785–789.
- [18] Jamróz, M.H. Vibrational Energy Distribution Analysis: VEDA 4 Program, Warsaw, 2004.
- [19] Sundaraganesan N, Ilakiamani S, Salem H, Wojciechowski PM, Michalska D. FT-Raman and FT-IR spectra, vibrational assignments and density functional studies of 5-bromo-2-nitropyridine. Spectrochim. Acta A 2005; 61; 2995-3001.

- [20] Sundaraganesan N, Ilakiamani S, Subramani P, Dominic Joshua B. Comparison of experimental and ab initio HF and DFT vibrational spectra of benzimidazole. *Spectrochimica Acta Part A* 2007: 67; 628-635.
- [21] Jamróz MH. Vibrational energy distribution analysis (VEDA): Scopes and limitations. *Spectrochimica Acta Part A* 2013: 114; 220-230.
- [22] Bürgi HB, Dunitz JD. Molecular conformation of benzylideneanilines; relation to electronic structure and spectra. *J. Chem. Soc. D*, 1969: 472-473.
- [23] Bernstein J. Conformational Studies. Part 111.1 Crystal and Molecular Structures of N-(2,4-Dichlorobenzylidene)aniline. *J Chem Soc Perkin Trans* 1972: 2; 946-950.
- [24] Vergoten G, Fleury G. Vibrational Spectroscopy Of Liquid Crystals 2. Normal Coordinate Analysis Of Benzaniline: Basis Structure For Some Liquid Crystals, *Journal of Molecular Structure* 1976: 30(2); 347-359.
- [25] Bernstein J, Schmidt GMJ. Conformational Studies. Part IV.1 Crystal and Molecular Structure of the Metastable Form of N-(p-Chlorobenzylidene)-p-chloroaniline, a Planar Anil, *J Chem Soc Perkin Trans* 1972: 2; 951-955.
- [26] Udhayakala P, Jayanthi A, Rajendiran TV, Gunasekaran S. Computation and interpretation of vibrational spectra, thermodynamical and HOMO-LUMO analysis of 2-chloro-4-nitroaniline. *Int J ChemTech Res* 2011: 3(4); 1851-1862.
- [27] Prasad JV, Rai SB, Thakur SN. Overtone spectroscopy of benzene derivatives using thermal lensing. *Chemical Physics Letters* 1989: 164(6); 629-634.
- [28] Hayd H, Savin H, Stoll A, Preuss H, Becker G. Influence of substituents on bond lengths. *Journal of Molecular Structure (Theochem)* 1988: 165; 87-97.
- [29] Gough KM, Henry BR. CH Stretching Overtone Spectra of Nitrobenzene and Its Deuterated Derivatives. Assignment of the Ortho CH. *J Phys Chem* 1989: 87; 3804-3805.
- [30] Mizugai Y, Katayama M, Nakagawa N. Substituent Effect on the Fifth Overtones of the Aryl C-H Stretching Vibrations in Disubstituted Benzenes. *J Am Chem Soc* 1981: 103; 5061-5063.
- [31] Traetteberg M, Hilmo I, Abraham RJ, Ljunggren S. The Molecular Structure Of N-Benzylidene-Aniline. *Journal of Molecular Structure* 1978: 48; 395-405.
- [32] Rukiah M, Lefebvre J, Descamps M, Hemon S, Dzyabchenko A. Ab initio structure determination of m-toluidine by powder X-ray diffraction. *J Appl Cryst* 2004: 37; 464-471.
- [33] Stuart B. *Infrared Spectroscopy: Fundamentals and Applications*. 2004: John Wiley & Sons, Inc. ISBNs: 0-470-85427-8 (HB); 0-470-85428-6 (PB).
- [34] Varsanyi G. *Assignments of Vibrational Spectra of Seven Hundred Benzene Derivatives*. Adam Hilger Ed. 1974: Vol. 1-2.
- [35] Silverstein M, Clayton Basseler G, Morill C. *Spectrometric Identification of Organic Compounds*. 2001: Wiley New York.

- [36] Kozhevina LI, Prokopenko EB, Rybachenko VI, Titov EV. Investigation Of Azomethine Group Vibrations In Aromatic Schiff Bases And Their N-Oxides By Vibrational Spectroscopy Methods. *Journal of Structural Chemistry* 1995; 36; 276-280.
- [37] Suydam FH. The C-N Stretching Frequency in Azomethines. *Analytical Chemistry*, 1963; 35(2); 193-195.
- [38] Meić Z, Baranović G. Vibrational Spectra of trans-N-Benzylideneaniline and Its Isotopomers. *Pure & Appl. Chem* 1989; 61(12); 2129-2138.
- [39] Campagnaro GE, Wood JL. The vibrational spectra and origin of torsional barriers in some aromatic systems. *Journal of Molecular Structure* 1970; 6; 117-132.
- [40] Figueroa AK, Peña CR, Campos-Vallette MM. Valence Force Constants of N-Benzylideneanilines. *Z Naturforsch* 1989; 44b; 923-927.
- [41] Tyagi P, Chandra S, Saraswat BS, Sharma D. Design, spectral characterization, DFT and biological studies of transition metal complexes of Schiff base derived from 2-aminobenzamide, pyrrole and furan aldehyde. *Spectrochimica Acta Part A: Molecular and Biomolecular Spectroscopy* 2015; 143; 1-11.
- [42] APEX2 and Saint, Bruker AXS 2007: Madison, Wisconsin, USA.
- [43] Sheldrick GM. SHELXS-97, Phase annealing in SHELX-90: direct methods for larger structures. *Acta Crystallogr* 1990; 46; 467-473.
- [44] Spek AL. Platon-A Multipurpose Crystallographic Tool Utrecht; Utrecht University 2005: The Netherlands.
- [45] Macrae CF, Edgington PR, McCabe P, Pidcock E, Shields GP, Taylor R, Oowler M Van de Streek. Mercury: visualization and analysis of crystal structures. *J Appl Crystallogr* 2006; 39; 453-457.